

Johnson Matthey's international journal of research exploring science and technology in industrial applications

\*\*\*\*\*Accepted Manuscript\*\*\*\*\*

## This article is an accepted manuscript

It has been peer reviewed and accepted for publication but has not yet been copyedited, house styled, proofread or typeset. The final published version may contain differences as a result of the above procedures

It will be published in the **July 2024** issue of the *Johnson Matthey Technology Review*

Please visit the website <https://technology.matthey.com/> for Open Access to the article and the full issue once published

## Editorial team

**Editor** Sara Coles

**Editorial Assistant** Aisha Mahmood

**Senior Information Officer** Elisabeth Riley

Johnson Matthey Technology Review  
Johnson Matthey Plc  
Orchard Road  
Royston  
SG8 5HE  
UK

**Tel** +44 (0)1763 253 000

**Email** [tech.review@matthey.com](mailto:tech.review@matthey.com)



<<https://doi.org/10.1595/205651324X17005622661871>>

<First page number: TBC>

## **Evaluation of Ammonia Co-fuelling in Modern Four Stroke Engines**

Ajith Ambalakatte

University of Nottingham, University Park, Nottingham, UK

Email: [ajith.ambalakatte@nottingham.ac.uk](mailto:ajith.ambalakatte@nottingham.ac.uk)

Abdelrahman Hegab

University of Nottingham, University Park, Nottingham, UK

Email: [abdelrahman.hegab@nottingham.ac.uk](mailto:abdelrahman.hegab@nottingham.ac.uk)

Sikai Geng

University of Nottingham, University Park, Nottingham, UK

Email: [sikai.geng@nottingham.ac.uk](mailto:sikai.geng@nottingham.ac.uk)

Alasdair Cairns

University of Nottingham, University Park, Nottingham, UK

Email: [alasdair.cairns1@nottingham.ac.uk](mailto:alasdair.cairns1@nottingham.ac.uk)

Anthony Harrington

MAHLE Powertrain Limited, Costin House, St. James Mill Road, Northampton, UK

Email: [anthony.harrington@mahle.com](mailto:anthony.harrington@mahle.com)

Jonathan Hall

MAHLE Powertrain Limited, Costin House, St. James Mill Road, Northampton, UK

Email: [jonathan.hall@mahle.com](mailto:jonathan.hall@mahle.com)

Mike Bassett

MAHLE Powertrain Limited, Costin House, St. James Mill Road, Northampton, UK

Email: [mike.bassett@mahle.com](mailto:mike.bassett@mahle.com)

<Article history>

PEER REVIEWED

Received 24th July 2023; Revised 1st November 2023; Accepted 15th November 2023; Online 21st November 2023

<End of article history>

**ABSTRACT**

Ammonia ( $\text{NH}_3$ ) is emerging as a promising alternative fuel for longer range decarbonised heavy transport, particularly in the marine sector due to highly favourable characteristics as an effective hydrogen carrier. This is despite generally unfavourable combustion and toxicity attributes, restricting end use to applications where robust health and safety protocols can be upheld. In the currently reported work, a spark ignited thermodynamic single cylinder research engine equipped with gasoline direct injection was upgraded to include gaseous ammonia port injection fuelling, with the aim of understanding maximum viable ammonia substitution ratios across the speed-load operating map. The work was conducted under overall stoichiometric conditions with the spark timing re-optimised for maximum brake torque at all stable logged sites. The experiments included industry standard measurements of combustion, performance and engine-out emissions (including  $\text{NH}_3$  "slip"). With a geometric compression ratio of 12.4:1, it was possible to run the engine on pure ammonia at low engine speeds (1000-1800rpm) at low-to-moderate engine loads in a fully warmed up state. When progressively dropping down below a threshold load limit, an increasing amount of gasoline co-firing was required to avoid engine misfire. Due to the favourable anti-knock characteristics, pure ammonia operation was up to 5% more efficient than pure gasoline operation under stable operating regions. A maximum net indicated thermal efficiency of 40% was achieved, with efficiency tending to increase with speed and load. For the co-fuelling of gasoline and ammonia in a pure ammonia attainable operating region, it was found that addition of gasoline improved the combustion, but these improvements were not sufficient to translate into

improved thermal efficiency. Emissions of  $\text{NH}_3$  slip reduced with increased gasoline co-fuelling, albeit with increased  $\text{NO}_x$ . However, the reduction in  $\text{NH}_3$  slip was nearly 10 times the increase in  $\text{NO}_x$  emissions. Comparing pure  $\text{NH}_3$  and pure gasoline operation,  $\text{NO}_x$  reduced by  $\sim 60\%$  when switching from pure gasoline to pure  $\text{NH}_3$  (as the latter is associated with longer and cooler combustion). Results were finally compared to those obtained a modern multi-cylinder Volvo "D8" turbo-diesel engine modified for dual fuel operation with ammonia port fuel injection, with the focus of the comparison being  $\text{NH}_3$  slip and  $\text{NO}_x$  emissions.

## 1. INTRODUCTION

The transportation sector is going through a renaissance in response to increasing pressures from global governments and society to reduce emissions of greenhouse gases and other pollutants resulting from the use of fossil fuels for power. While electrification is often considered the preferred solution to tackle this challenge, relative immaturity of battery technology, combined with associated lack of energy density, make full electric propulsion unsuitable for heavy transport applications such as marine, off-road, rail and freight.

Ammonia ( $\text{NH}_3$ ) has gained significant interest in recent years, both as a decarbonised energy vector and efficient hydrogen carrier. Volumetrically, liquid  $\text{NH}_3$  can store  $\sim 45\%$  more hydrogen than liquid hydrogen. Furthermore,  $\text{NH}_3$  can be inexpensively stored as liquid (at  $-33^\circ\text{C}$  at 0.1MPa or 0.86MPa at  $15^\circ\text{C}$ ) and conveniently transported. Such promising characteristics of  $\text{NH}_3$  have led many researchers to believe ammonia could become a key fuel for heavy transport, provided

that key challenges around slow combustion and emissions control can be overcome [1,2].

## 2. RELATED WORK

Due to the versatility of ammonia and the renewed interest, significant research is being carried out in all forms of powerplants including fuel cells, gas turbines in addition to internal combustion engines. However, most of the research on gas turbines are confined to power generation, where ammonia is blended with conventional fuels to reduce the carbon output [3–7]. The concept of using  $\text{NH}_3$  as a fuel in internal combustion engines can be traced back nearly a century, where it was used to run buses in Belgium during the 2nd World War [8]. This was followed by extensive research in the mid-1960s, where experiments were carried out in both Compression Ignition (CI) and Spark Ignition (SI) engines. Due to the high auto ignition temperature of  $\text{NH}_3$ , pure ammonia operation in CI engines is only possible with very high compression ratios (e.g.  $\sim 35:1$ ) [9]. As a result, most studies in CI engines focus on “dual fuel” operation, where a pre-mixed ammonia-air mixture is ignited by a pilot fuel of low auto ignition temperature and favourable cetane rating.

The dual fuel approach has been extensively researched with various fuels including diesel, dimethyl ether, kerosene and amyl-nitrate [10–17]. Most of these studies tried to achieve Homogenous Charge Combustion Ignition (HCCI) using early injection of pilot fuel, which often lead to poor substitution ratios of ammonia and increased emissions of Carbon monoxide (CO), unburned hydrocarbons and ammonia. A strategy involving auto ignition of pilot-fuel to increase the cylinder temperatures were also studied by Zhang et al [18] and Lee et al [19], the former used this strategy

to vaporise liquid ammonia in low speed 2 stroke engine which resulted in improved efficiency and emissions compared to pure diesel operation, in case of the latter, this strategy was implemented in 35:1 compression ratio engine to enable monofuel operation with just ammonia, however this strategy was never realised experimentally.

However, the added complexity of an additional fuel circuit, coupled with difficulties in operating the engines under throttled conditions and the inability to operate the engine with pure ammonia at lower compression ratio makes this solution less attractive compared to SI engines. Compared to compression ignition, pure ammonia operation can be achieved in SI engines at considerably lower compression ratios as reported by Starkman et al. as early as the 1960s [20]. Pearsall et al. [15] investigated the operation with ammonia in both types of engines and recommended a high compression ratio (e.g. [12-16]) SI engine as an ideal solution.

While better than compression ignition, the relatively poor premixed combustion characteristics of  $\text{NH}_3$  (see Table 1) make it challenging to operate a SI engine with pure  $\text{NH}_3$  at low loads. However, several strategies can be considered, such as increasing the effective compression ratio, supercharging (potentially without charge-air cooling), high ignition energy and co-fuelling with a faster burning sustainable fuel(s). Of these solutions, co-fuelling with hydrogen has been more extensively studied due to excellent combustion characteristics combined with the potential ability to produce the hydrogen onboard via  $\text{NH}_3$  "cracking".

Morch et al. [21] investigated the combustion of  $\text{NH}_3$  at different hydrogen substitution levels and concluded that  $\sim 10\%$  volume substitution yielded maximum thermal efficiency. Further to this, Firgo et al. [22] investigated ammonia-hydrogen

co-fuelling at various speed/load conditions and concluded that combustion improvement from hydrogen enrichment had reduced impact on engine speed extension compared to engine load. They further calculated the minimum amount of hydrogen energy required for stable combustion to be roughly ~7% for full load and ~11% for part load conditions. These researchers also investigated the feasibility of using exhaust gas heat to crack  $\text{NH}_3$  on board and confirmed that hydrogen can be produced via the solution, however, the higher combustion temperatures required for the cracker resulted in significantly higher  $\text{NO}_x$  emissions [23]. Recently investigations conducted Lhuillier et al. [24] and Mounaïm-Rousselle et al. [25] in modern SI engines also concluded that the combustion of  $\text{NH}_3$  can be greatly improved by small amounts of hydrogen (~10% vol) allowing the engine to operate at various loads and engine speeds ranging from 650 to 2000rpm.

**Table 1 Combustion Characteristics of Ammonia and Hydrogen compared to conventional fuels** [26–30]

Species	Hydrogen	Ammonia	Gasoline	Diesel
Chemical Formula	$\text{H}_2$	$\text{NH}_3$	$\text{C}_n\text{H}_{1.87n}$	$\text{C}_n\text{H}_{1.8n}$
LHV [MJ/kg]	120	18.8	44	42.5
Laminar Burning Velocity @ $\lambda=1$ [m/s]	3.51	0.07	0.45	0.3
Auto-ignition Temperature [K]	773-850	930	~623	~533
Research Octane Number	>100	130	90-99	40-60
Flammability Limit in Air [vol. %]	4-75	15-28	1-7.6	0.6-5.5
Quenching Distance [mm]	0.9	22.07	1.98	-
Absolute Minimum Ignition Energy [mJ]	0.02	8	0.3	0.2

Gasoline has also been studied extensively as a combustion promoter for  $\text{NH}_3$  in SI engines, notably investigated by the CFR research group. Grannell et al. [31] investigated the fuel limits and efficiency of ammonia-gasoline co-fuelling and

concluded that ammonia can replace most of the gasoline energy above 4bar IMEPn, with the amount of gasoline needed reducing with increasing engine load and speed. Interestingly, their work with various compression ratios didn't yield improvements in gasoline displacement or thermal efficiencies. Ryu et al. [32] investigated the direct injection of gaseous NH<sub>3</sub> into a Port Fuel Injected (PFI) gasoline engine and concluded that the long injection times needed for NH<sub>3</sub> negated any benefits of direct injection compared to PFI systems [33]. These researchers further conducted experiments with direct injection of cracked ammonia and found that the exhaust heat can be used to crack NH<sub>3</sub> on board without having significant impact on the performance and emissions of the engine. Haputhanthri et al. [34] studied the combustion of ammonia/gasoline emulsified mixtures and found that ammonia can be dissolved into gasoline using emulsifiers like ethanol and methanol and that the composite fuel was capable of improving the performance of engine at high load conditions.

However, most published work introduces ammonia via fumigation reducing the accuracy of identifying the maximum viable substitution of ammonia, in the current reported work ammonia was injected using a dedicated port fuel injector minimising any errors with ammonia consumption. This enabled the identification of maximum viable substitution of ammonia over a speed and load points in an operating map by using E10 co-fuelling at points where pure ammonia operation was not possible. The goal was to undertake a baseline analysis in a modern high performance gasoline engine equipped with a modern combustion chamber layout and durable high energy ignition system designed for highly downsized SI engines (e.g. >30bar IMEP). The



study was also extended to direct comparison with dual fuel operation in a modern diesel engine still capable of full diesel “fallback” operation.

### 3. EXPERIMENTAL SETUP

#### Engine Hardware

For NH<sub>3</sub> co-fuelling with E10 testing, the experiments were undertaken in an externally boosted SI research engine, which was a single cylinder derivative of the MAHLE Powertrain “DI3” demonstrator engine. The engine was equipped with a central spark plug and side mounted gasoline direct injector located under the intake valves for delivering standard UK pump grade gasoline (E10). Ammonia was delivered at the port via an upgraded manifold using a prototype Clean Air Power port fuel injector. The engine was also equipped with hydraulic fully independent variable valve timing to enable optimisation of valve timing and overlap. Set out in Table 2 are the key characteristics of the engine.

**Table 2 SI Engine hardware specifications**

Parameters	Value
Engine Type	Four Stroke Single Cylinder Spark Ignition
Displaced Volume [cc]	400
Stroke [mm]	83
Bore [mm]	73.9
Compression Ratio	12.39
Number of Valves	4
Valvetrain	Dual Independent Variable Valve Timing (40°CA Cam Phasing)
Fuel Injection Configuration	Side DI Gasoline (E10) PFI Ammonia
Max Fuel Injection Pressure [bar]	175 (gasoline)
Cylinder Head Geometry	Pent-Roof (high tumble port)
Piston Geometry	Pent-Roof with Cut-outs for Valves

Ignition Coil	Single Fire Coil, 100mJ, 30kV
Max Power [kW]	40 (gasoline)
Max IMEPn [bar]	30 (gasoline)
Max In-cylinder Pressure [bar]	120
Max Speed [rpm]	5000
Boost System	External Compressor (Max 4bar Absolute)
Control System	MAHLE Flexible ECU
Interface Software	ETAS INCA

Schematics of the intake air system and the ammonia supply system are shown in Figures 1 and 2, respectively. The engine could be operated as either naturally aspirated or boosted using an external compressor rig providing up to 4 barA boost pressure. The temperatures of intake air (45°C), engine coolant (95°C) and oil (95°C) were maintained at a constant value ( $\pm 1^\circ\text{C}$ ) using dedicated conditioning circuits. Furthermore, surge tanks were added to both the intake and exhaust to minimise the effects of unwanted gas pressure fluctuations.

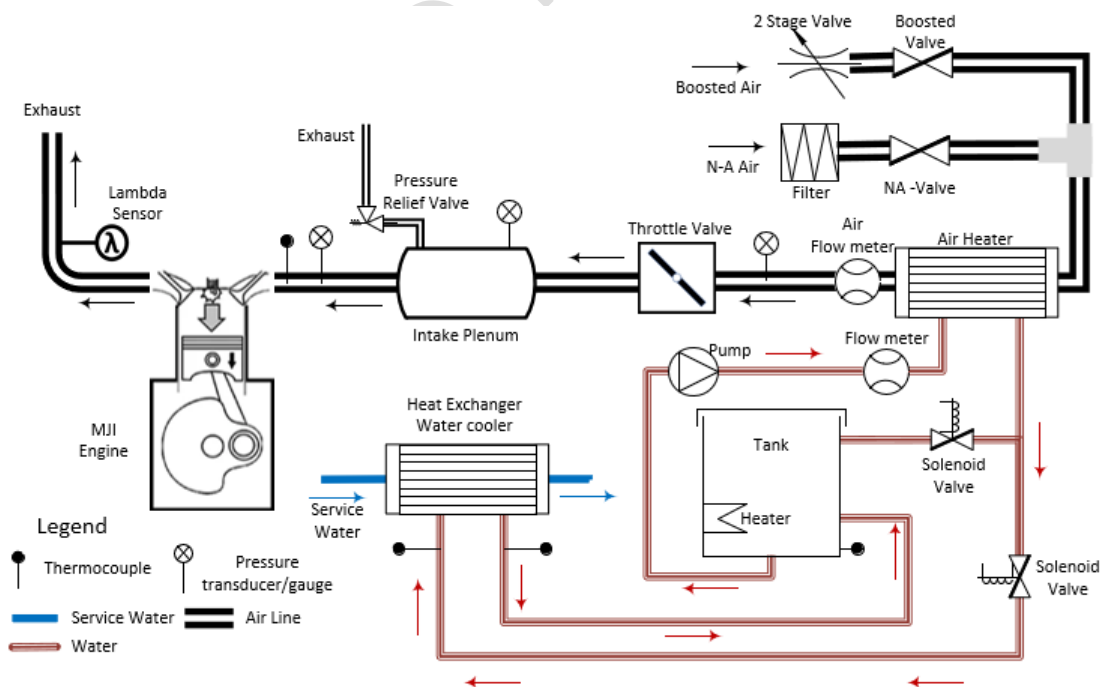


Fig. 1 Schematic of the test rig gas path and coolant control

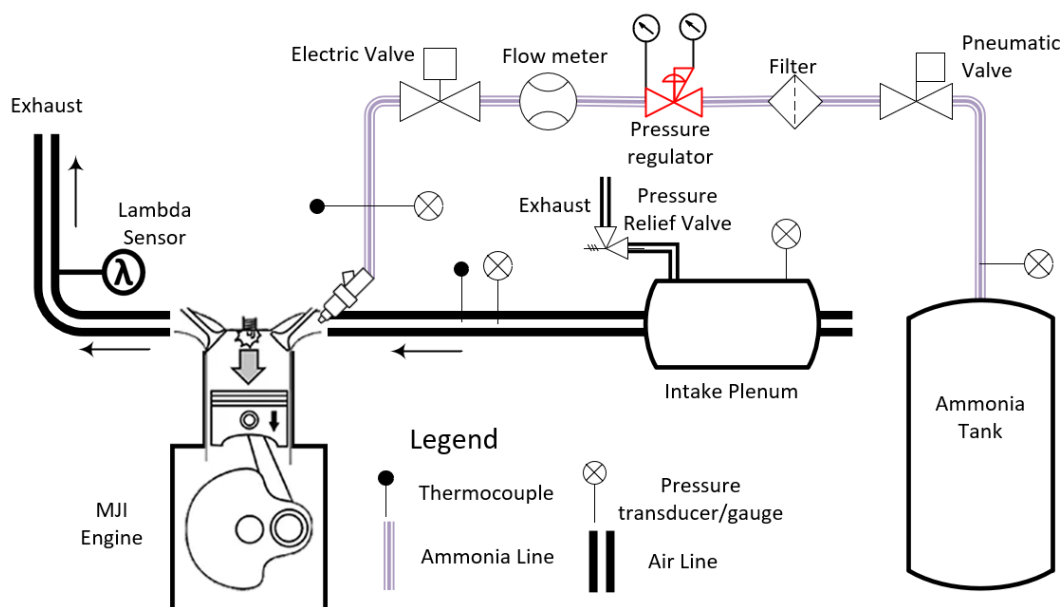


Fig. 2 Schematic of the engine fuel supply line

The ammonia was supplied to the engine in gaseous phase using a dedicated port injector supplied by Clean Air Power. The  $\text{NH}_3$  was stored as liquid-vapour at equilibrium in a 530kg drum, with the pressure differential between the intake manifold and vapour pressure inside the drum used to drive the supply of ammonia to engine. The flowrate of  $\text{NH}_3$  was measured using a high-accuracy micro-motion Coriolis flowmeter (maximum flow rate error of 1% at the minimum flow rates reported). Electrically controlled safety valves and nitrogen-based purging were added to the supply line to isolate the ammonia supply in the case of an emergency. For the gasoline supply, an AVL 735 fuel balance unit was used to measure the gasoline (E10) flowrate and condition the gasoline temperature (20°C set point) before being fed to a high-pressure fuel pump at constant supply pressure via a fuel regulator.

In-cylinder pressure was measured using a Kistler 6045-B piezoelectric pressure transducer working through an AVL Micro-FEM amplifier, and fully calibrated to industry standards via a dead weight tester. The intake and exhaust pressures were

also measured using Kistler's 4045A and 4011 piezo resistive transducers. The engine-out emissions were measured using a series of dedicated analysers from the Signal group, in addition to industry standard emissions (NO<sub>x</sub>, CO<sub>2</sub>, CO, THC and O<sub>2</sub>) ammonia "slip" emissions (unburned NH<sub>3</sub> in the exhaust) were also measured based on a new Signal unit. The details of the emission analysers are summarised in Table 3. All measurements were recorded and processed using a bespoke National Instruments Data Acquisition system. In-cylinder pressure data were recorded at a resolution of 0.2 Crank Angle degrees (CAD) using a Hohner 3232 optical encoder for 300 consecutive cycles. A one-dimensional heat release model was used to estimate the mass fraction burned.

**Table 3 Details of the emission analysers**

Equipment	Gas	Operating Principle	Dynamic Range (Volume)	Accuracy / Error (%)
4000 VM	NO <sub>x</sub>	Chemiluminescence	0-1000 ppm	Better than +1% range or ±0.2 ppm whichever is greater.
8000 M	O <sub>2</sub>	Dumbbell paramagnetic sensing	0 -5 %, 0 -10 %, 0 -25 %	±0.01 %O <sub>2</sub> .
S4 Nebula	NH <sub>3</sub>	Tuneable Diode laser Spectrometry	1ppm -10,000 ppm	±2% of FDS
3000 HM	THC	Flame ionisation detector	0-10000 ppm	Better than ±1 % range or ±0.2 ppm whichever is greater.
7000 FM	CO, CO <sub>2</sub>	Infra-red gas filter correlation technique	100-10000 ppm Or 1-100 %	Better than ±1 % of range or ±0.5 ppm whichever is greater.

For NH<sub>3</sub>-diesel dual-fuel (DF) testing, the experiments were conducted using a Volvo Penta 235kW in-line 6-cylinder 7.7-litre high-pressure common-rail (HPCR) production diesel engine, retrofitted for dual-fuel operation with gaseous NH<sub>3</sub> port injection (six injectors, one per each cylinder, also supplied by Clean Air Power) and equipped with the same industry standard measurements of performance, fuel consumption and exhaust gas emissions. The main specifications of the engines are set out in Table 4. The same Ammonia system used with the SI engine was employed to supply gaseous NH<sub>3</sub> to the engine, via a directional three-way valve and independent metering and control unit.

**Table 4 Main specifications of the multi-cylinder Volvo engine used in the NH<sub>3</sub>-diesel dual fuel testing**

Engine model	Volvo Penta TAD873VE
No. of cylinders	6 Cylinders, Inline
Engine displacement (L)	7.7
Rated power (kW)	235 @ 2200 rpm
Rated torque (Nm)	1310 @ 1450 rpm
Cooling system	Water cooled
Induction system	Exhaust Gas Turbocharged, Intercooled
EGR system	Electronically controlled EGR system
Stroke [mm]	110
Bore [mm]	135
Compression ratio	17.5:1
Number of valves per cylinder	4 (2 intake; 2 exhaust)
Fuel injection system	For diesel fuel: High-pressure common-rail (HPCR) direct injection (DI) For Ammonia: Port Injection (PFI)
Max Fuel Injection Pressure [bar]	Diesel Fuel: 2400 bar NH <sub>3</sub> : 10 bar
Diesel fuel to conform to	EU EN590US D975, 1-D and 2-D

### Test plan (Spark Ignition)

Since practical applications of ammonia are expected to be in low-to-medium speed heavy duty engines, the test points were selected to cover typical peak power-speed ratings. The tests were conducted at 1000, 1400 and 1800rpm with the engine load varied from 4 to 12 bar net Indicated Mean Effective Pressure (IMEP<sub>n</sub>). The aim of the tests was to determine the pure ammonia speed-load map and associated impacts upon combustion, performance, fuel economy and emissions with and without co-fuelling. The co-fuelling required was evaluated by undertaking ammonia “displacement sweeps”, with the engine first fired using pure E10, then NH<sub>3</sub> was progressively added until an upturn in the combustion stability occurred (with repeat logs around this upturn to establish the maximum possible NH<sub>3</sub> substitution, while the upper limit was set to a coefficient of variation in IMEP of >3%). All logs were obtained under stoichiometric conditions with the spark timing set to Maximum Brake Torque (MBT). In early work it was proposed that slightly rich running might aid NH<sub>3</sub> displacement (due to slightly higher laminar burning velocity) but this was not found to be the case; with the engine misfiring more easily when attempting to operate slightly richer when at the substitution ratio limit due to the relatively low relative air-to-fuel ratio of NH<sub>3</sub> and significant reduction in the ratio of specific heats (and hence gas temperature) “over-ruling” relatively small increases in laminar burning velocity when slightly rich [35].

The engine settings used for the tests are set out in Table 5. The valve timing was fixed for the tests, however, the overlap was adjusted from 37° to 24° CA for the 1000rpm tests, as the slow speed combined with high boost pressure otherwise would

have resulted in significant ammonia slip, due to the high apparent cylinder scavenging at this speed.

**Table 5 Engine settings for substitution tests**

Settings	Values
Operating Temperature (Coolant & Oil) [ $^{\circ}\text{C}$ ]	95
Spark Timing	Maximum Brake Torque (MBT)
Air-fuel Equivalence ratio	1
E10 Injection Start angle [CAD BTDCf]	310
Ammonia Injection End angle [CAD BTDCf]	400
Inlet air temperature [ $^{\circ}\text{C}$ ]	45
Ammonia rail pressure [barG]	3-5
Ammonia Feed Temperature [ $^{\circ}\text{C}$ ]	27 - 30
E10 Temperature [ $^{\circ}\text{C}$ ]	20

#### Test plan (Dual Fuel)

$\text{NH}_3$ -diesel dual-fuel tests were carried out at a fixed engine speed of 600rpm (the minimum engine speed; to help with the slow combustion of ammonia), with load sweeps between half and full load conditions. Throughout the testing, the diesel fuelling quantity was kept constant, while the load was increased via increasing the  $\text{NH}_3$  quantity; the substitution ratio (%SR) of  $\text{NH}_3$  for diesel fuel was calculated accordingly as a percent of the  $\text{NH}_3$  used to the total fuel (energy basis). All the experiments were carried out at fully-warm conditions and un-throttled operation. The main test conditions of the engine are summarised in Table 6.

**Table 6 Main test conditions for the  $\text{NH}_3$ -diesel dual fuel experiments**

Engine speed (rpm)	600
Engine Load – MEPn (bar)	5 -10
Rated load at the test speed (%)	47 - 97
Diesel fuel flowrate (kg/hr)	4 (fixed)
$\text{NH}_3$ flowrate (kg/hr)	0 - 11 (changing)

#### 4. RESULTS

##### Maximum Displacement of Ammonia (Spark Ignition)

The results of the maximum ammonia percent displacement at various test points are shown in Figure 3.

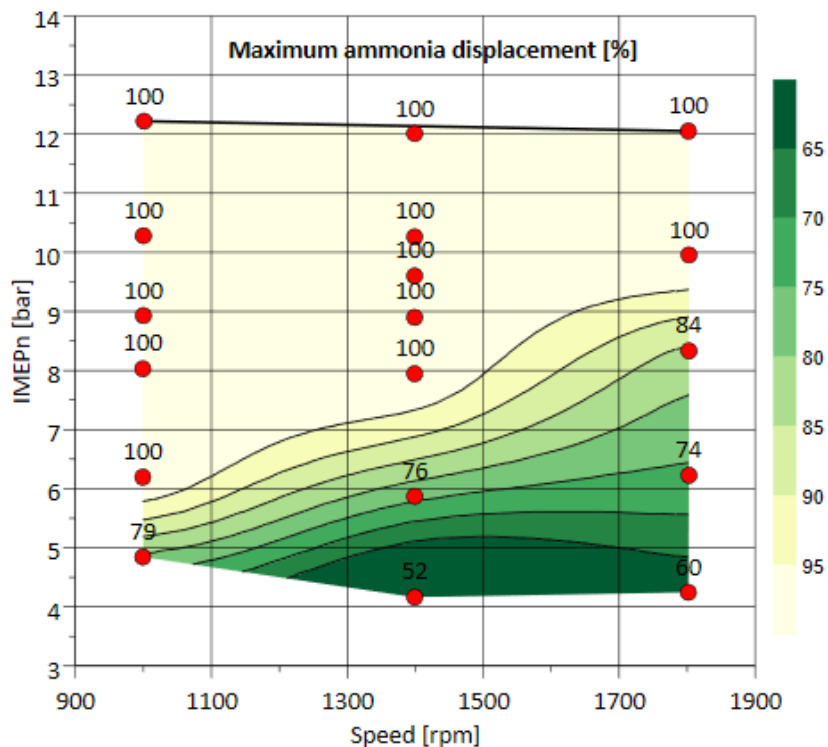


Fig. 1. Maximum substitution of ammonia achieved at different load points ( $\lambda=1$ , MBT spark timing)

The engine was capable of operating with pure  $\text{NH}_3$  at relatively moderate engine loads. Furthermore, ammonia constituted most of the fuel energy across the map, validating the prior findings of Granell et al. [31]. The 100% substitution isoline follows a near-linear pattern, with the threshold load required to operate on pure  $\text{NH}_3$  increasing by 2bar IMEP for an increase of 400rpm in engine speed. This direct relation of threshold engine load and engine speed was also observed by Mounaïm-Rousselle et al. [25] in their work on ammonia SI engines. This trend is despite increasing gas



temperatures at higher speeds and illustrates the dominance in lower speed providing more time for combustion to occur despite the fact the in-cylinder and exhaust gas temperatures usually increase with engine speed (for a given load). The impact of increasing in-cylinder turbulence with higher speed remains unknown and will be studied in future work.

### General Trends of Ammonia Combustion in SI engines

#### Combustion

Figure 4 shows the spark timing required to achieve MBT and the corresponding stability of the engine at the tested points. Examining the map, it is evident that the engine operation improves considerably as the load increases from the threshold load for pure ammonia operation.

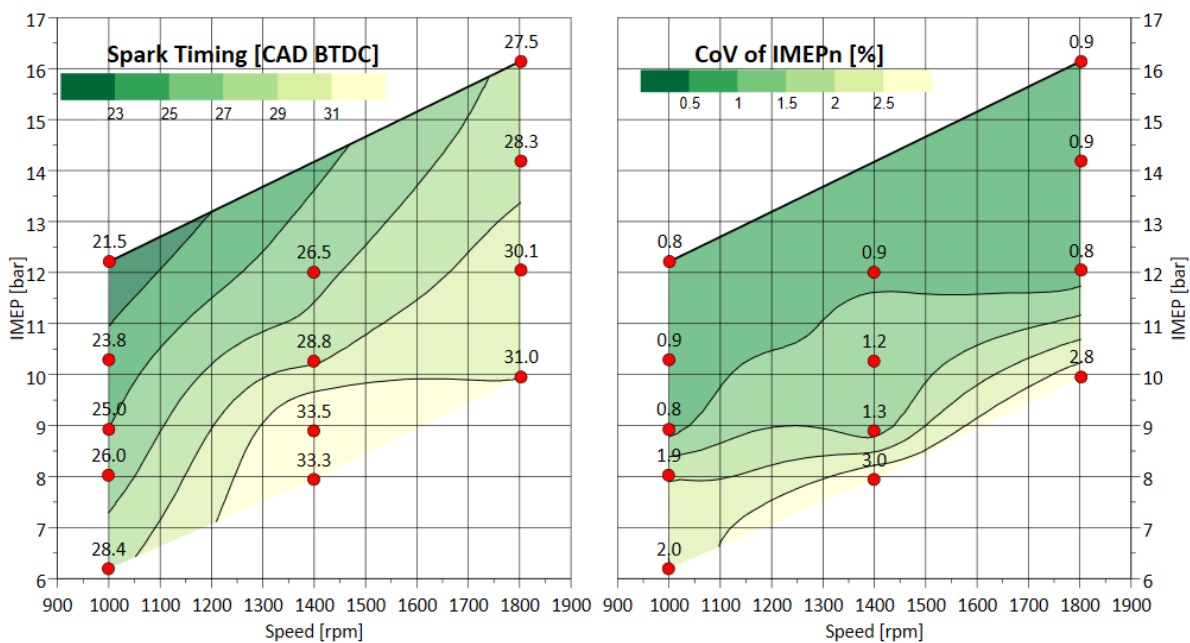


Fig. 2. Spark timing and CoV of IMEPn of pure ammonia test points

The spark advance required to achieve MBT reduces with increase in load or reduction in engine speed, similarly the engine operation becomes notably more stable

beyond 4bar IMEPn at all engine speeds. The mass fraction burned at the various test points is shown in Figure 5, where the “flame development phase” (0%-10% MFB) followed a similar trend to the spark timing. However, the “combustion phase” (10%-90% MFB) variation was relatively smaller for the test points. Moreover, the flame development phase was similar to the combustion phase at low speeds and became larger than the combustion phase as the speed increased. In other words, nearly 50% or more of the total combustion duration encompasses the flame development phase. The lack of variation in the combustion phase with speed could be a direct result of increased turbulence enabled by a high tumble head used in the study (to be confirmed in future optical and CFD analysis work).

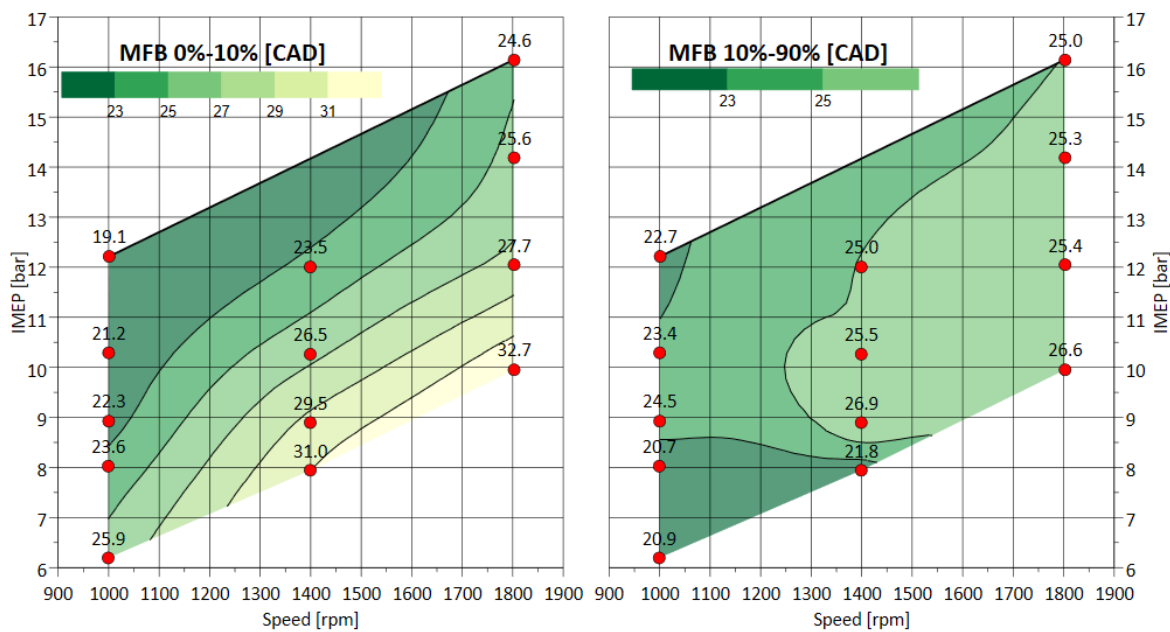


Fig. 3. Variation of combustion metrics 0%-10% MFB and 10%-90% MFB for pure ammonia combustion at various speeds and loads

## Efficiency

The variation in net Indicated Thermal Efficiency (ITE) in the test region for pure NH<sub>3</sub> operation and pure E10 operation is set out in Figure 6. Pure NH<sub>3</sub> operation is considerably more efficient than E10 in the test region by virtue of ammonia having a high-octane rating and low air-fuel ratio, both of which combined enabled the engine to be operated at MBT with high loads, allowing the engine to achieve efficiencies as high as 40% at 1800rpm/16bar IMEPn.

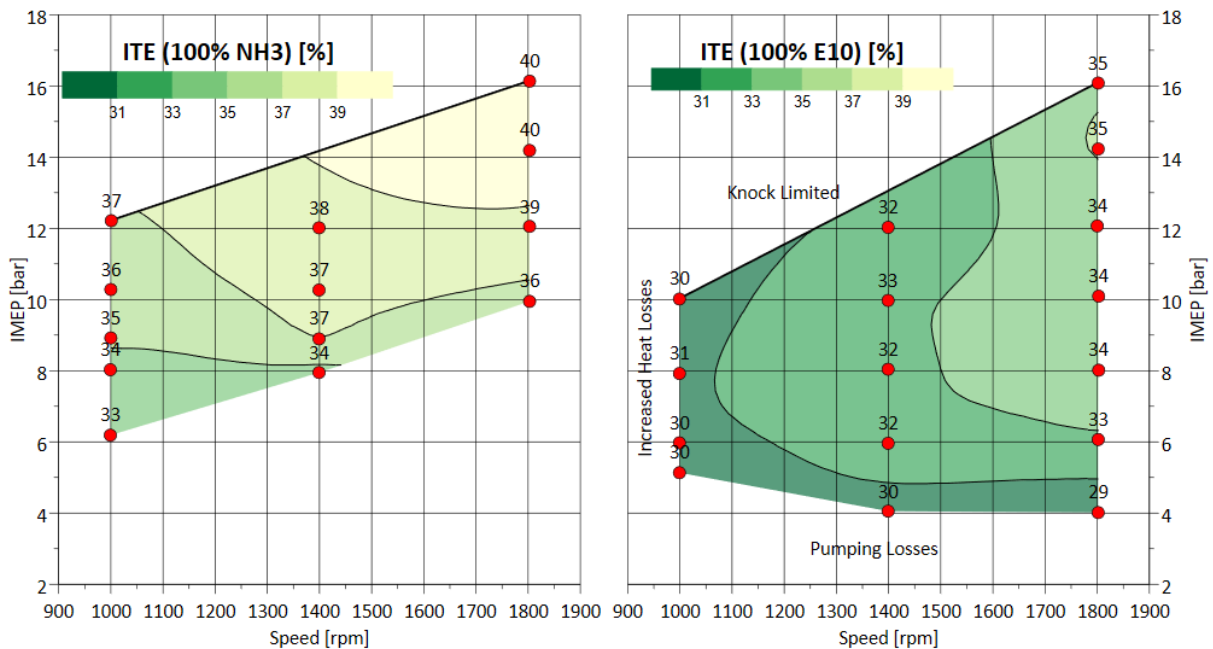


Fig. 4. ITE of 100% NH<sub>3</sub> vs 100% E10 operation

Examining the variation of ITE for pure NH<sub>3</sub> operation, the efficiency improves with increase in speed and load, where the impact of load increase is larger than that of engine speed. This variation suggests that the losses from increased heat rejection, pumping and knock (that govern E10 operation in the test region) do not directly apply to (or have minimal impact on) pure NH<sub>3</sub> operation.

## Emissions

The NO<sub>x</sub> and NH<sub>3</sub> slip emissions from the engine operating on pure NH<sub>3</sub> are set out in Figure 7. NO<sub>x</sub> emissions remain relatively similar across the tested region, with the values increasing closer to the threshold load points mainly due to the advanced spark timing aiding the NO<sub>x</sub> formation via increased cylinder temperature. However, the emissions are nearly a third of that produced during pure E10 operation (~3000-4000ppm) under the same conditions.

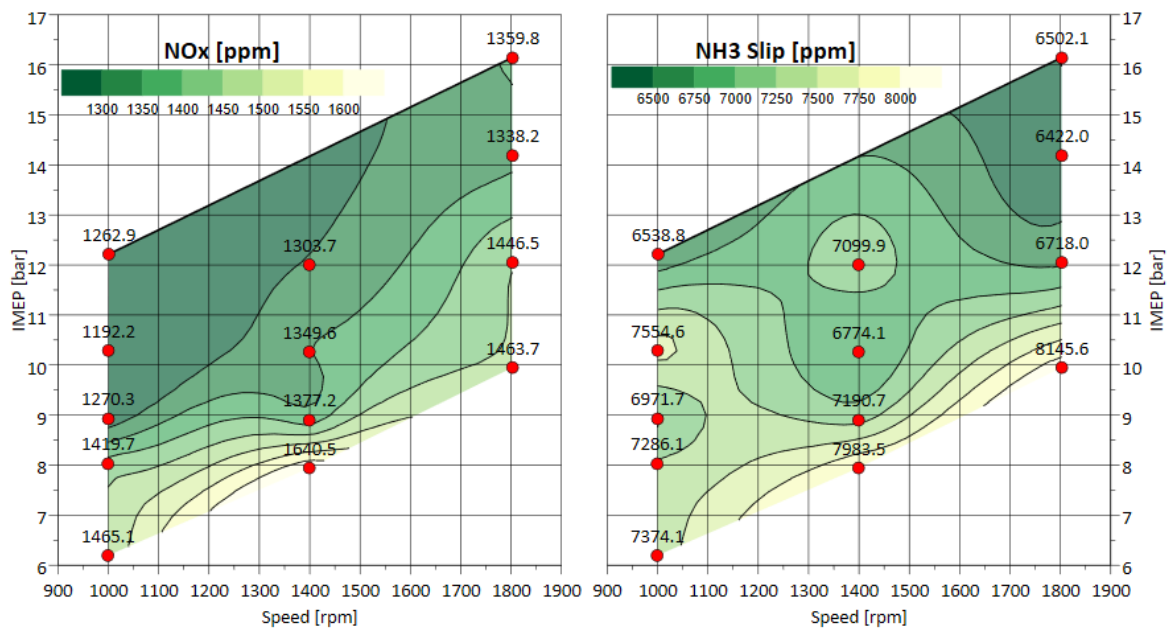


Fig. 5. Emissions of NO<sub>x</sub> and ammonia slip for pure ammonia test region

Similar to NO<sub>x</sub>, ammonia slip also peaks near the threshold load from the unstable engine operation in those points. While the slip improves with engine stability, there is considerable slip (> 0.5% vol) even in the stable operating points. The recorded NH<sub>3</sub> slip values are comparable to previous studies published by Lhuillier et al and Mounaïm-Rousselle et al [24,36] using similar engines and under similar operating conditions ( $\lambda$ , MBT). The two major causes for the high values of slip are (a)

in-cylinder scavenging, pushing part of the injected ammonia in the intake port directly into the exhaust and (b) the incomplete combustion of ammonia trapped in crevice volumes. However, further investigations are necessary to quantify such effects. One of the potential uses of the excessive slip is to clean the NO<sub>x</sub> via a Selective Catalytic Reduction (SCR) catalyst, potentially eliminating the need for any "AdBlue" (to be confirmed in future work). Moreover, high exhaust gas temperatures could enable the oxidation of excess ammonia within the catalyst as determined by Girard et al [37]. However, the "alpha" ratio (ratio of NH<sub>3</sub> to NO<sub>x</sub> in ppm) is considerably higher than desired values between 1 and 2, which suggests the need for ammonia scrubber/oxidation catalyst to remove the excess ammonia (with potential trade-offs to be made with N<sub>2</sub>O production).

#### E10-Ammonia Co-fuelling at High Load Conditions

As explained in the previous section, while pure NH<sub>3</sub> operation can be achieved at moderate-to-high load operation, some form of fuel enhancement is needed to stably operate the engine at low loads, idling and cold start. Therefore, additional displacement tests were conducted at a pure NH<sub>3</sub> operational starting point with the aim of understanding if co-fuelling enhances the performance, efficiency or emissions of the engine (despite the fact pure ammonia operation was possible). The tests were conducted at 1400rpm and 10bar IMEP<sub>n</sub> with the engine settings as previously listed in Table 4.

### Combustion

The impact of increased E10 substitution on the stability and spark timing of the engine is shown in Figure 8. Replacing 25% of the energy with E10 improves the

stability as well as the spark advance required to achieve MBT. Further substitution of E10, however, did not have any positive impact on the operation of the engine. A similar pattern can also be found with addition of NH<sub>3</sub> to pure E10 operation. the high knock resistance of NH<sub>3</sub> allows the engine to be operated at MBT without knock suppression improving the stability of operation.

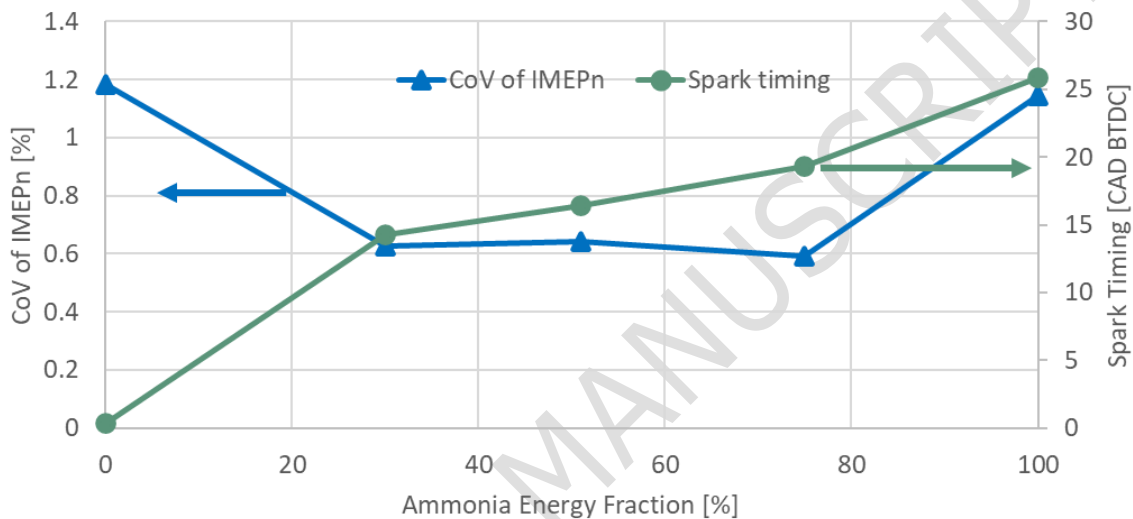


Fig. 6. Stability and MBT Spark timing for different levels of E10 substitution

The impact of E10 substitution on mass fraction burned is depicted in Figure 9, where the addition of 25% E10 reduces the flame development phase of combustion by 25%. However, further increase in substitution had reducing impact on the flame development phase. Similar results were also obtained by Mercier et al. [38] in their studies with hydrogen substitution, however, the similar substitution of hydrogen (10-15%) had a bigger impact (~50%) than E10.

Compared to the flame development phase, E10 substitution had minimal impact on the combustion, taking a similar duration as the pure ammonia combustion. Ammonia substitution, however, increases the combustion phase considerably as

indicated by increase in values between 0% and 30%. This data showed no benefits in combustion can be achieved by increasing the substitution beyond ~25%.

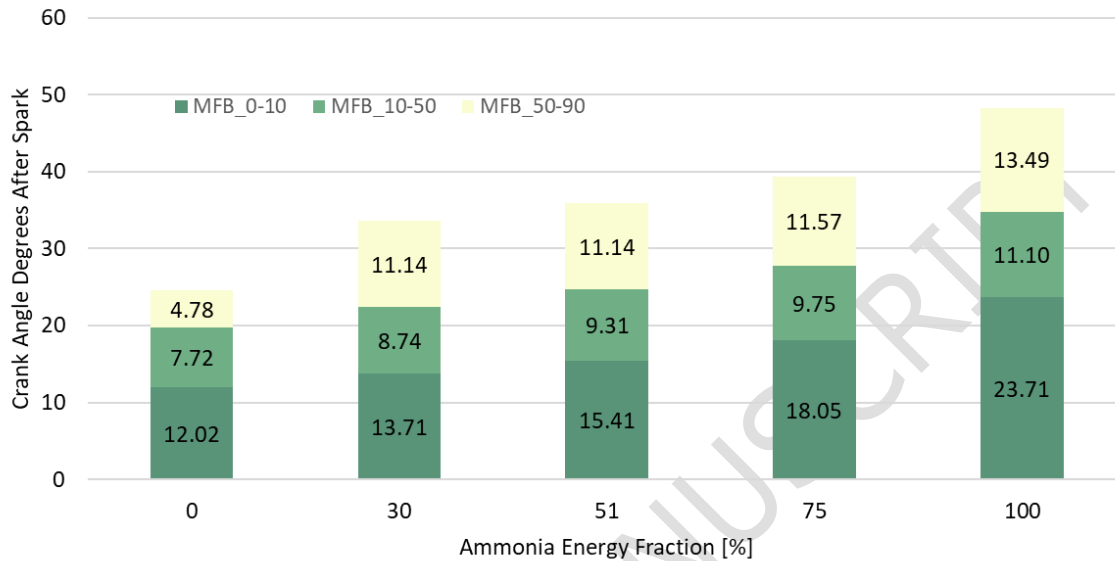


Fig. 7. Combustion metrics for different levels of ammonia substitution

## Efficiency

The values of ITE achieved at different substitution rates are shown in Figure 10, where addition of E10 to the engine reduces the efficiency, however the impact is less than 1% and remains nearly constant in the co-fuelling region. This indicates that the improvements in combustion achieved from E10 substitution increases the ratio of heat losses to work output.

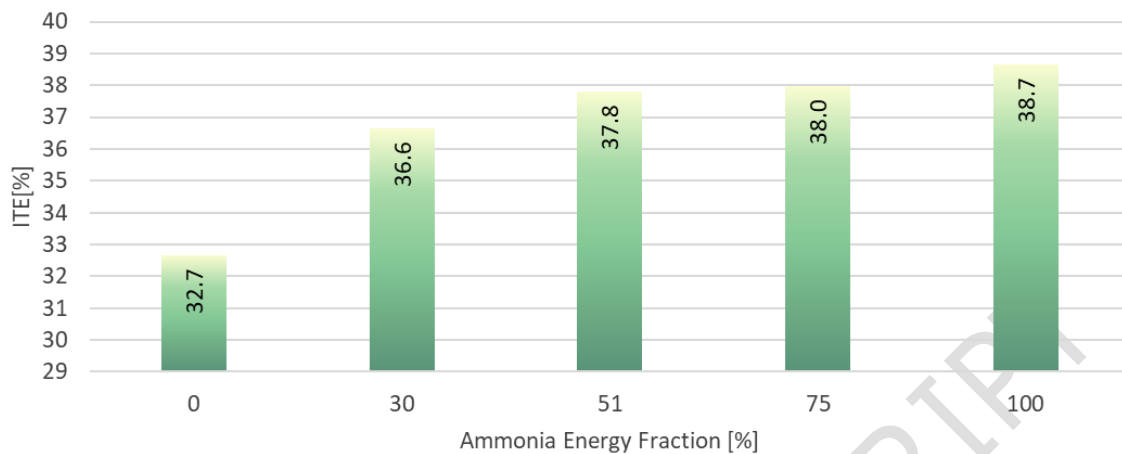


Fig. 8. Indicated thermal efficiency achieved at different E10 substitution rates

## Emissions

The impact of E10 co-fuelling on NO<sub>x</sub> and NH<sub>3</sub> slip is shown in Figure 11. While co-fuelling with E10 would add other carbon-based emissions they are not shown here as these emissions simply increased in linear proportion to increased E10 substitution. Compared to pure NH<sub>3</sub> operation, co-fuelled operation decreases the NH<sub>3</sub> slip considerably, partially due to the lower quantities of NH<sub>3</sub> injected and resulting higher cylinder temperatures, as is evident from the increase in NO<sub>x</sub> values with increased substitution.



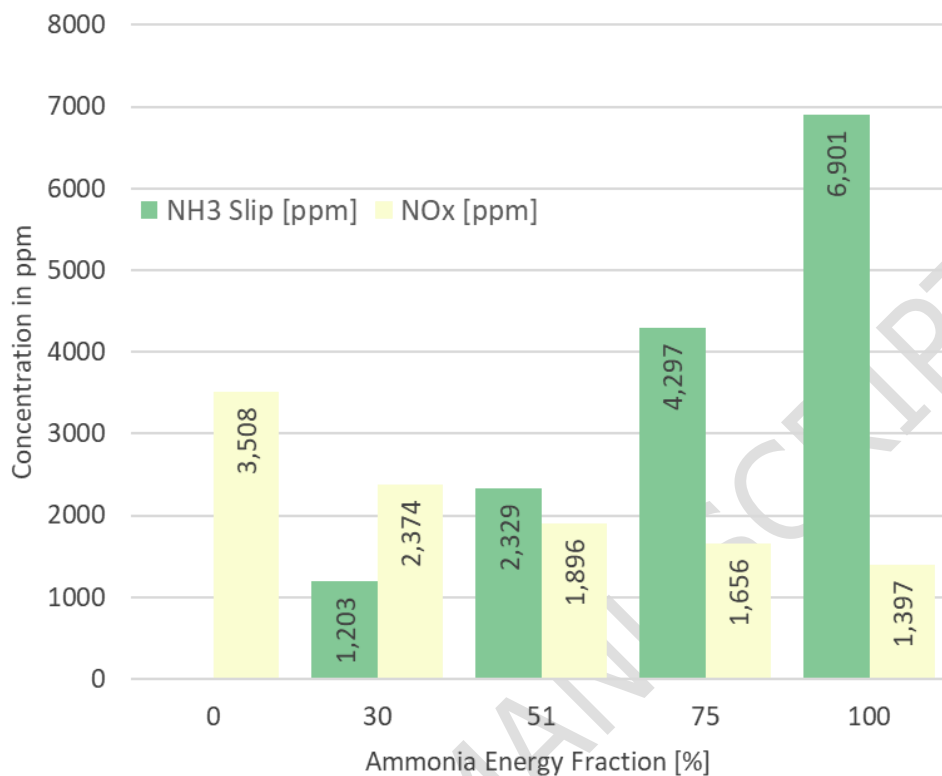


Fig. 9. Emissions of NO<sub>x</sub> and ammonia slip for various E10 substitution rates

Comparing the values of NH<sub>3</sub> slip and NO<sub>x</sub> emissions, the drop in NH<sub>3</sub> slip emissions is nearly 10 times that the increase of NO<sub>x</sub> between each level of substitution. Furthermore, comparing pure NH<sub>3</sub> and pure E10 operation, the NO<sub>x</sub> emissions reduce by nearly 60% from 3500ppm to 1400ppm.

These tests indicate that co-fuelling in the pure NH<sub>3</sub> capable operating region can deliver positive impacts with respect to combustion and emissions without affecting the efficiency considerably. Further investigations with more reactive fuels like hydrogen could yield better results and will be investigated in future work.

#### Ammonia-Diesel Dual-Fuel Operation

As mentioned before, the focus of the comparison between the SI engine data and that of the NH<sub>3</sub>-diesel dual fuel engine was to assess the NH<sub>3</sub> slip and how this

correlated to engine-out NO<sub>x</sub> emissions. Set out in Figure 12 are the absolute values of NH<sub>3</sub> slip and NO<sub>x</sub> emissions (in ppm). Corresponding data for NH<sub>3</sub> fuel flow rate and the resulting substitution ratio of NH<sub>3</sub> for diesel fuel (%SR) is illustrated in Figure 13. It can be seen that at low %SR (below 50%), the NH<sub>3</sub> slip increases as the amount of NH<sub>3</sub> admitted to the cylinder increases. This indicates that NH<sub>3</sub> combustion under these conditions is relatively incomplete. At these conditions, NO<sub>x</sub> emissions are decreased, potentially due to the cooling effect of the NH<sub>3</sub> being admitted into the cylinder in multiphase form.

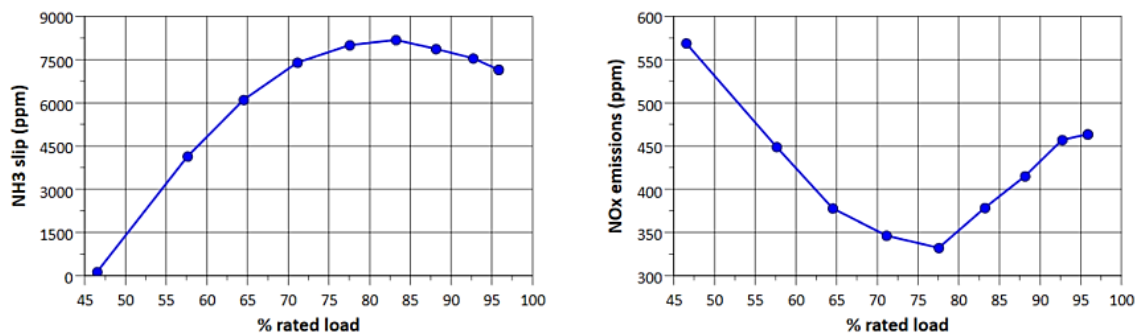


Fig. 12. NH<sub>3</sub> slip and NO<sub>x</sub> emissions (ppm) for dual-fuel operation

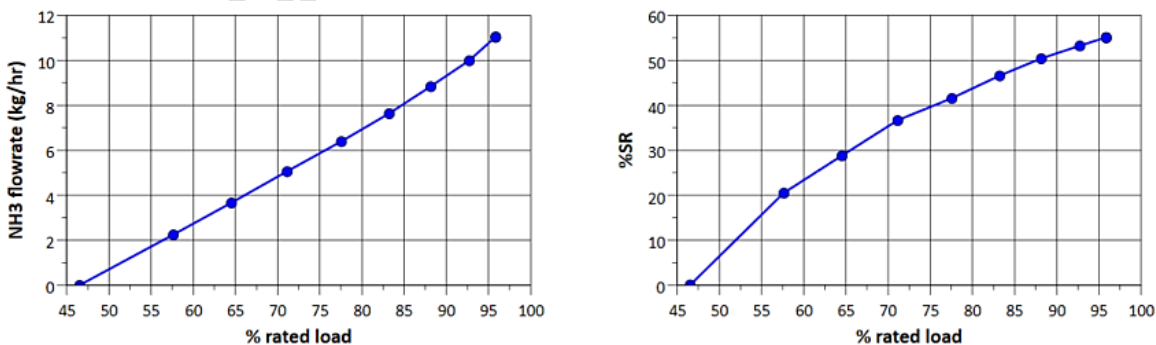


Fig. 13. NH<sub>3</sub> flowrate (kg/hr) and the corresponding substitution ratio (%) for dual-fuel operation

The trends in increasing  $\text{NH}_3$  and reducing  $\text{NO}_x$  emissions trends were crudely maintained with increasing load until around 80% load, with reversing trends observed at higher loads. The incident of inversion indicates that the increased fuel-air mixture strength, as more  $\text{NH}_3$  is admitted into the cylinder, substantiates the combustion, and hence  $\text{NH}_3$  slip decreases. The improved combustion also occurs at higher temperature, which promotes the formation of more thermal  $\text{NO}_x$  (despite the cooling effect of the  $\text{NH}_3$ ), although its value remains inferior to those under conventional diesel operation.

The improved ammonia combustion is also evident by the improved engine stability; also occurring around the threshold. It has been found that such a threshold was attained slightly leaner than stoichiometric conditions ( $\sim \lambda=1.25$ ); with the corresponding lambda curve and the engine stability indicator (as expressed by the Coefficient of Variation (COV) of the IMEPn) presented in Figure 14.

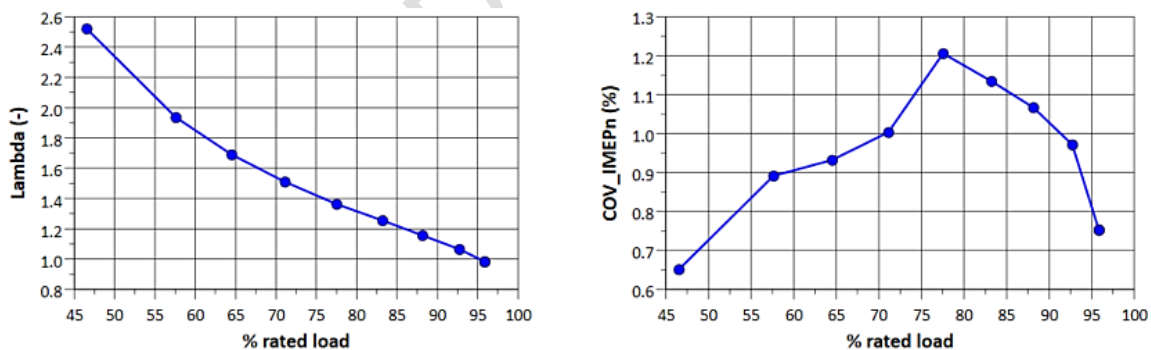


Fig. 14. Lambda (-) and COV of IMEPn (%) for dual-fuel operation tests

Although the presence of gaseous  $\text{NH}_3$  in the exhaust gas improves the  $\text{NO}_x$  conversion efficiency of the Selective Catalytic Reduction (SCR), the optimal ratio of the  $\text{NH}_3$  to  $\text{NO}_x$  (aka alpha -  $\alpha$ ) ranges between 1 to 1.4 in most applications. The values obtained

from the current work excessively exceeded that; these must be fully converted for NH<sub>3</sub>-diesel DF engines to be viable. This will require ammonia oxidation catalysis to also be adopted in future dual fuel applications.

## 5. Conclusions

The study examined the engine behaviour and emissions of pure ammonia and ammonia-E10 co-fuelling under low speeds and a fully warm engine state. The findings revealed that pure ammonia can be used efficiently at low to moderate loads, with the minimum load for stable operation decreasing with lower engine speed. Co-fuelling with E10 was required for stable operation below the minimum load, but most test points achieved more than 50% ammonia substitution. The spark timing for best combustion improved with increasing load from the minimum point. The flame development phase of pure ammonia combustion was equal to or longer than the combustion phase, and both phases varied with load and speed changes. Pure ammonia operation led to higher net indicated thermal efficiency and lower NO<sub>x</sub> emissions than pure E10 operation, due to the beneficial anti-knock and low-temperature combustion associated with ammonia.

The study also investigated the effect of E10 as a fuel enhancer, by conducting co-fuelling studies in pure ammonia operating region, which showed a improvement in both stability of operation and combustion speed. The main effect of E10 was on the flame development phase of the combustion reducing the duration by 5 CAD for a 25% substitution. However, the improvements in combustion doesn't translate into improved efficiency, which decreased by 1% for the substitution. E10 co-fuelling also

impacts the emissions with NO<sub>x</sub> increasing and ammonia slip decreasing, with the impact of co-fuelling diminishing beyond 25% substitution.

The work was complemented with an investigation of the NH<sub>3</sub> slip and NO<sub>x</sub> emissions in a NH<sub>3</sub>-diesel Dual Fuel (DF) heavy duty engine. The results show generally a higher NH<sub>3</sub> slip than SI engines at a given speed and load. Unlike conventional diesel engines, NH<sub>3</sub>-Diesel DF engines need to operate near stoichiometric conditions for improved stability, performance and reduced NH<sub>3</sub> slip. However, running in stoichiometric conditions leads to poor efficiency (e.g. part throttle operation at low loads leading to higher pumping losses). Lastly, the slip from NH<sub>3</sub>-Diesel DF operation were considerably higher than the optimum amount needed for reducing NO<sub>x</sub> in a SCR, suggesting the need for ammonia aftertreatment in NH<sub>3</sub>-diesel DF engines.

Immediate future work focusses on gaining a better understanding of the same accompanied by detailed breakdown of NO<sub>x</sub> species (NO, N<sub>2</sub>O, NO<sub>2</sub>) at varied compression ratios and relative fuel to air ratios. The engine is also being modified to incorporate a longer stroke to bore ratio to enable operation with higher compression ratios that replicate the operation of a heavy-duty engine.

## 6. Acknowledgements

The authors would like to acknowledge the financial support of the EPSRC. The authors would also like to thank Clean Air Power for their support in providing the ammonia injectors and the Lab Technicians for their hard work and dedication to ensure the safety of all personnel in the lab.

## References

- [1] IRENA, A Pathway to Decarbonise the Shipping Sector by 2050, 2021.  
Johnson Matthey Technol. Rev., 2024, **68**, (3), xxx-yyy Page 28 of 32  
<<https://doi.org/10.1595/205651324X17005622661871>>

- [2] APC UK, Thermal Propulsion Systems Technology Indicators and Drivers, 2020.
- [3] M. Guteša Božo, M.O. Viguera-Zuniga, M. Buffi, T. Seljak, A. Valera-Medina, *Appl Energy* 251 (2019) 113334.
- [4] A. Valera-Medina, M. Gutesa, H. Xiao, D. Pugh, A. Giles, B. Goktepe, R. Marsh, P. Bowen, *Int J Hydrogen Energy* 44 (2019) 8615–8626.
- [5] D. Pugh, A. Valera-Medina, P. Bowen, A. Giles, B. Goktepe, J. Runyon, S. Morris, S. Hewlett, R. Marsh, *Proceedings of the ASME Turbo Expo 4A-2020* (2021).
- [6] A. Valera-Medina, D.G. Pugh, P. Marsh, G. Bulat, P. Bowen, *Int J Hydrogen Energy* 42 (2017) 24495–24503.
- [7] F.J. Verkamp, M.C. Hardin, J.R. Williams, *Symposium (International) on Combustion* 11 (1967) 985–992.
- [8] Korch Emerio, *Journal of Institute of Petroleum* 31 (1945) 213–223.
- [9] J.T. Gray, E. Dimitroff, N.T. Meckel, R.D. Quillian, *SAE Transactions* 75 (1967) 785–807.
- [10] K. Ryu, G.E. Zacharakis-Jutz, S.C. Kong, *Appl Energy* 113 (2014) 488–499.
- [11] C.W. Gross, S.C. Kong, *Fuel* 103 (2013) 1069–1079.
- [12] S.S. Gill, G.S. Chatha, A. Tsolakis, S.E. Golunski, A.P.E. York, *Int J Hydrogen Energy* 37 (2012) 6074–6083.
- [13] A.J. Reiter, S.C. Kong, *Fuel* 90 (2011) 87–97.
- [14] A.J. Reiter, S.C. Kong, *Energy and Fuels* 22 (2008) 2963–2971.
- [15] T.J. Pearsall, C.G. Garabedian, *SAE Transactions* 76 (1968) 3213–3221.

- [16] M. Pochet, V. Dias, H. Jeanmart, S. Verhelst, F. Contino, *Energy Procedia* 105 (2017) 1532–1538.
- [17] K.L. Tay, W. Yang, J. Li, D. Zhou, W. Yu, F. Zhao, S.K. Chou, B. Mohan, *Appl Energy* 204 (2017) 1476–1488.
- [18] Z. Zhang, W. Long, P. Dong, H. Tian, J. Tian, B. Li, Y. Wang, *Fuel* 332 (2023) 126086.
- [19] D. Lee, H.H. Song, *Journal of Mechanical Science and Technology* 2018 32:4 32 (2018) 1905–1925.
- [20] E.S. Starkman, H.K. Newhall, R. Sutton, T. Maguire, L. Farbar, *SAE Transactions* 75 (1967) 765–784.
- [21] C.S. Mørch, A. Bjerre, M.P. Gøttrup, S.C. Sorenson, J. Schramm, *Fuel* 90 (2011) 854–864.
- [22] S. Frigo, R. Gentili, *Int J Hydrogen Energy* 38 (2013) 1607–1615.
- [23] S. Frigo, R. Gentili, F. De Angelis, *SAE Technical Papers* 2014-November (2014).
- [24] C. Lhuillier, P. Bréquigny, F. Contino, C. Mounaïm-Rousselle, *Fuel* 269 (2020).
- [25] C. Mounaïm-Rousselle, A. Mercier, P. Brequigny, C. Dumand, J. Bourriot, S. Houillé, C.M. Mounaïm-Rousselle, *International Journal of Engine Research* (2021) 146808742110387.
- [26] J.R. Grove, *Institute of Chemical Engineers* 25 (1968).
- [27] P. Dimitriou, R. Javaid, *Int J Hydrogen Energy* 45 (2020) 7098–7118.
- [28] C. Lhuillier, P. Brequigny, F. Contino, C. Rousselle, *SAE Technical Papers* (2019).



- [29] A.P.L. Robinson, D.J. Strozzi, J.R. Davies, A. Kumamoto, H. Iseki, R. Ono, T. Oda, *J. Phys.: Conf. Ser* 301 (2011) 12039.
- [30] M. Ciniviz, H. Köse, *International Journal of Automotive Engineering and Technologies* 1 (2012) 1–15.
- [31] S.M. Grannell, D.N. Assanis, S. V. Bohac, D.E. Gillespie, *J Eng Gas Turbine Power* 130 (2008).
- [32] K. Ryu, G.E. Zacharakis-Jutz, S.C. Kong, *Appl Energy* 116 (2014) 206–215.
- [33] K. Ryu, G.E. Zacharakis-Jutz, S.C. Kong, *Int J Hydrogen Energy* 39 (2014) 2390–2398.
- [34] S.O. Haputhanthri, C. Austin, T. Maxwell, J. Fleming, *IOSR Journal of Mechanical and Civil Engineering (IOSR-JMCE)* 11 (2014) 11–18.
- [35] H. Kobayashi, A. Hayakawa, K.D.K.A. Somarathne, E.C. Okafor, *Proceedings of the Combustion Institute* 37 (2019) 109–133.
- [36] C. Mounaïm-Rousselle, P. Bréquigny, C. Dumand, S. Houillé, *MDPI* (2021).
- [37] J. Girard, R. Snow, G. Cavataio, C. Lambert, *SAE Technical Papers* (2007).
- [38] A. Mercier, C. Mounaïm-Rousselle, P. Brequigny, J. Bouriot, C. Dumand, *Fuel Communications* 11 (2022) 100058.

### The Authors



Dr Ajith Ambalakatte is a post-doctoral researcher in the Powertrain Research Centre at the University of Nottingham, leading experimental research into next generation high efficiency ammonia and hydrogen fuelled internal combustion engines under the EPSRC “MariNH3” programme (<https://marinh3.ac.uk/>). His prior direct experience includes research into novel



	ammonia production and storage working with global industry partners.
	Dr Abdelrahman Hegab is a Senior Research Fellow in the Powertrain Research Centre at the University of Nottingham. He is an expert in advanced dual fuel internal combustion engines for future decarbonised heavy power, with prior direct experience across dual fuel natural gas, hydrogen and ammonia propulsion. He is currently leading the development of a novel “flexi-fuel” dual fuel engine platform under the Research England “Hydex” programme ( <a href="https://hydex.ac.uk/">https://hydex.ac.uk/</a> ).
	Professor Alasdair Cairns is the Director of the Powertrain Research Centre at the University of Nottingham, with over 23 years’ experience in low carbon fuels and propulsion systems in both industry and academia. He is the Programme Director of the EPSRC “MariNH3” programme investigating ammonia fuelled engines for future marine applications. He has led over 30 previous funded projects with several global industry partners, published over 95 related international publications and previously won prizes for research from the IMechE, IEEE and SAE International.